



Spatiotemporal analysis of national carbon emission and regional carbon simulation in China

Yuxiang Cheng¹ · Yuqi Tang^{1,2} · Bin Zhou^{1,2} · Huihui Feng^{1,3}

Received: 7 September 2023 / Accepted: 28 December 2023 / Published online: 11 January 2024
© The Author(s), under exclusive licence to Springer-Verlag GmbH Germany, part of Springer Nature 2024

Abstract

Land use and land cover (LULC) will cause large flows of carbon sources and sinks. As the world's largest carbon emitter with a complicated LULC, China's carbon emissions have profound implications for its ecological environment and future development. In this paper, we account for the land-use changes and carbon emissions of 30 Chinese provinces and cities in China from 2000 to 2020. Furthermore, the spatial correlation of carbon emissions among the study areas is explored. Four typical regions with spatial association (Beijing, Hebei, Sichuan, and Anhui) are selected, and their land-use change trends in 2025 and 2030 are simulated to predict the total carbon emissions in the future. The results show that the distribution of land-use in China is mainly cultivated and woodland, but the growth of urban built-up (UBL) land area indirectly leads to the continuous increase of carbon emissions. Total carbon emissions have increased over the past two decades, albeit at a slower growth rate, with some provinces experiencing no further growth. In the typical regional carbon emission simulation, it is found that the carbon emissions of the four provinces would show a downward trend in the future. The main reason is the reduction in indirect carbon emissions from fossil energy in UBL, while the other part is the influx of carbon sinks due to grassland, woodland, etc. We recommended that future carbon reduction measures should focus and prioritize controlling fossil energy and mitigating carbon emissions from UBL. Simultaneously, the significant contribution of forests and other land types as carbon sinks should be acknowledged to better implement China's carbon neutral commitment.

Keywords Land use and land cover (LULC) · Carbon emission · Dual carbon goals · Spatial analysis · Carbon simulation

Introduction

Human activities, including deforestation (Lorenz and Pitman 2014), agricultural land reclamation, accelerated urbanization, overgrazing of grasslands and pollution of water bodies, have significantly impacted Land use and land cover (LULC) (Hong et al. 2021). LULC

is an important factor that leads to carbon emissions and determines the spatiotemporal carbon transfer in terrestrial ecosystems (Piao et al. 2009), in which the effect of construction and cultivated lands are dominant (Lai et al. 2016; Zhang et al. 2020, 2023). Urban built-up land (UBL) carbon emissions primarily result from burning fossil energy, while cultivated land emissions arise from CO₂ and CH₄ indirectly released during crop production (Chuai et al. 2011). Therefore, LULC change has aggravated the global greenhouse gas emissions and ecosystem anomaly (Smith et al. 2008; Wang and Myint 2016). The 6th reports of Intergovernmental Panel on Climate Change (IPCC) indicates that global average surface temperature has risen by about 1 °C between 1850 and 1900, and this trend is expected to accelerate in the coming decade (Houghton 2003; IPCC Climate Change 2022; Wang et al. 2014). With LULC change and fossil energy consumption rising from human activities, total carbon emissions of China are constantly increasing. It accounts for about 27.5% of global carbon dioxide emissions, surpassing the USA as

Responsible Editor: V.V.S.S. Sarma

✉ Yuqi Tang
yqtang@csu.edu.cn

¹ School of Geosciences and Info-Physics, Central South University, Changsha 410083, China

² Key Laboratory of Spatio-Temporal Information and Intelligent Services, Ministry of Natural Resources, Changsha 410083, China

³ Key Laboratory of Urban Land Resources Monitoring and Simulation, Ministry of Natural Resources, Shenzhen 518000, China

the largest carbon emitting country (Dong et al. 2019; Yang et al. 2019). China needs to reasonably manage and control its land-use distribution structure and fossil energy consumption to achieve its emission reduction policy.

Therefore, analysis of the LULC change and fossil energy consumption can reveal the rate of human-induced carbon emissions in China (Li et al. 2020). It is of great significance in guiding China in the critical stage of achieving the goal of “dual carbon”. And it will further have a positive effect on slowing down the global greenhouse gas emissions and climate and environmental changes.

A large amount of literature has discussed the relationship between LULC change and carbon emissions (Chuai et al. 2015; Guo et al. 2019; Jung et al. 2012; Li et al. 2022b; Mallik et al. 2022; Pechanec et al. 2018). The carbon stocks of different land-use types change as they are converted from one type to another. Carbon stocks in Jiangsu decreased by 714.03×10^4 t between 1995 and 2015, and the land transfer of cultivated land to urban land is the main land transfer causing the carbon sequestration loss (Guo et al. 2019). Moreover, the carbon sequestration increases 9.74Tg during the ecological conservation of Fujian Province, which is mainly caused by vegetation conversion (Li et al. 2022b). On the other hand, it is found that the carbon sequestration capacity varies among ecosystems, and the carbon sequestration and carbon emissions are spatially and temporally heterogeneous based on LULC distribution in the same ecosystem (Le Quere et al. 2009; Luysaert et al. 2008; Zhao et al. 2023). Consequently, carbon emissions from LULC changes in Jiangxi show evident spatial heterogeneity, characterized by concentrated high emissions in the north and low emissions in the south, creating areas with lighter and heavier emissions, respectively (Huang et al. 2023). Carbon emissions are spatially concentrated in northwestern China and follow a “northeast-southwest” trend, with the center of emissions shifting northward over time. The dominant characteristic of regional carbon emissions is a low total amount, low intensity, and low pressure (LLL) (Han et al. 2021).

Analyzing the impact of LULC changes on carbon sources and sinks is crucial for future ecosystem structure protection (Tao et al. 2015). Studies have emerged on the simulation of future carbon emissions. While some studies estimate future ecosystem carbon emissions based on the current situation (Houghton and Hackler 2003; Li et al. 2022a; Yang et al. 2018), others predict these emissions using land use simulation models (Brovkin et al. 2013; Liang et al. 2021b; Molotoks et al. 2018). Using a cultivated land expansion prediction model, it is projected that Brazil and Mexico will lose about 13.7% and 4.6% of their vegetation and soil carbon stocks, respectively (Molotoks et al. 2018). In the future, forests in the tropical dry forests of western Zambia will hold larger carbon stocks compared to agricultural land. The soil carbon pool of agricultural land will be

able to offset about 33% of the loss of carbon stocks due to deforestation (Dietz et al. 2023).

In addition, some literature discussed the calculation of the regional carbon sequestration and emissions. It usually calculates the carbon sequestration by the net primary productivity (NPP) or the vegetation carbon density, while estimate the urban carbon emissions through the nighttime lighting data (Field et al. 1998; He et al. 2016; Su et al. 2014). However, due to inconsistencies in the magnitudes of carbon sources and sinks, there is no unified standard for calculating regional carbon sequestration and emissions.

In previous literature, the impacts are generally analyzed by blindly choosing local regions, without being able to recognize China’s overall carbon situation. And the literature generally simulates carbon emissions separately for land-use or fossil energy, with few articles analyzing and predicting them in parallel. Therefore, considering the existence of some of the above problems, this paper selects the partial hinterland of China to study the national impacts of LULC change and fossil energy consumption on carbon emissions firstly. And choosing the typical regions via spatial correlation to predict the emission changes in the future. Then we introduce urban carbon density to jointly simulate carbon emission for land-use types and fossil energy to compensate for some weaknesses in the existing literature. The results of this study can offer insights into emission reduction measures informed by the historical effects of LULC on carbon emissions and spatio-temporal distribution in China, and provide some guidance for regional carbon emission prediction.

Methods and materials

Study region and data preparation

China’s land area is about 9.6 million km², and its sea area is about 4.73 million km². China’s land resources utilization is complex due to the diverse natural conditions and unique historical development in various regions. China’s land resources are currently unevenly distributed, leading to various national and regional problems. For example, forest resources are limited. In the northeastern forest areas, efforts are underway to balance harvesting and cultivation, while the southwestern forest areas are grappling with an abundance of over-mature trees and resource wastage. China’s vast grassland resources remain underutilized, resulting in low levels of livestock production. However, many local grasslands are struggling with overgrazing and pasture degradation. Limited cultivated land is predominantly found in the eastern monsoon zone plains, whereas most grassland resources are located in the eastern part of the Inner Mongolia Plateau.

Considering the uneven distribution of the population, land-use and carbon fluxes, as well as data availability, 30 provinces and municipalities in China's partial hinterland (excluding Tibet, Hong Kong, Macao, Taiwan, and South China Sea Islands) are chosen as the study area for this paper.

The datasets used in this study mainly consist of land-use data, energy consumption and other data on driving factors. The land cover product data between 2000 and 2020 are used at 5-year intervals. The energy consumption data is obtained from the China Energy Statistical Yearbook, which has been

converted to units of standard coal. The Digital Elevation Model (DEM), road, population and other driving factor data were harmonized to the WGS-84 coordinate system. Among them, land-use data and energy consumption data were used to calculate land-use carbon sources and sinks, while driving factor data was used for land-use change prediction. The specific data information is shown in Table 1.

Methodology

This study consists of three main parts (Fig. 1). Firstly, we estimate national level carbon emissions and sequestrations using land-use data and fossil energy consumption data, and analyze their spatiotemporal distribution from 2000 to 2020. Next, we identify spatial correlations of carbon emissions among provinces and analyze their spatial distribution patterns. Subsequently, we select some typical regions based on their distinct carbon emission spatial characteristics compared to neighboring ones, and the driving factors are analyzed and predict their carbon emissions in 2025 and 2030 with the PLUS model.

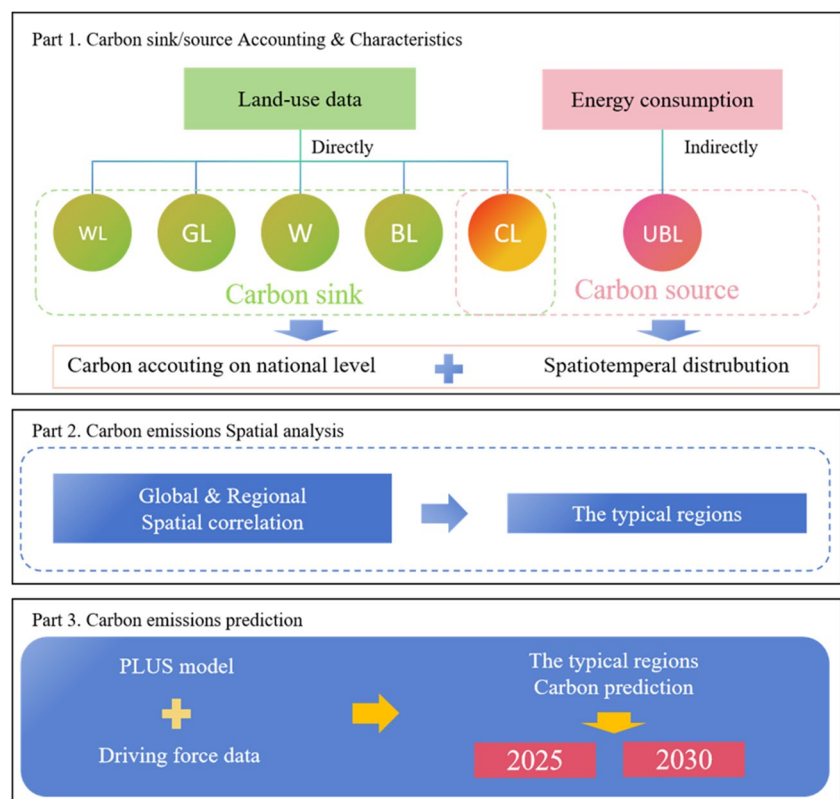
Carbon sequestration/source accounting

In this paper, we resampled and reclassified the original land use data to a spatial resolution of 1 km for easier data processing. We divided the land use types into six categories:

Table 1 Data description

| Data | Resolution | Types | Data source |
|---|-------------|------------|---|
| Land-use data | 30 m × 30 m | Raster | CLCD (Yang and Huang 2021) |
| Energy data | - | Panel data | China Statistical Yearbook |
| DEM | 30 m × 30 m | Raster | Geospatial Data Cloud (https://www.gscloud.cn/) |
| River Rail Road | - | Shapefile | Open Street Map (OSM) |
| Temperature Precipitation Population GDP | 1 km × 1 km | Raster | Chinese Academy of Sciences (https://www.resdc.cn/) |

Fig. 1 The research framework (CL: cultivated land; WL: woodland; GL: grassland; W: water; UBL: urban built-up land; BL: bare land)



cultivated land, woodland, grassland, water, urban built-up land and bare land. Among the six land use types, cultivated land, woodland, grassland, water and bare land exhibit direct carbon flux, allowing them to exchange carbon with the environment. However, the carbon emission of urban built-up land is calculated based on energy consumption, and cannot directly interact with carbon flux (Chuai et al. 2015). Direct carbon emissions from land uses can be estimated using the widely accepted IPCC carbon emission method (1).

$$C_D = \sum_i^n Area_i * \epsilon_i \tag{1}$$

where C_D represents the direct carbon emission (t). $Area_i$ and ϵ_i represent the area (km²) and carbon emission/sequestration coefficient of the corresponding i th land-use type. According to the researches on carbon source and sequestration of different land uses in China, the carbon emission/sequestration coefficients are shown in Table 2.

Since urban built-up land cannot exchange carbon fluxes directly with the environment, we estimate carbon emissions based on fossil energy consumption, following the IPCC method. The energy sources included in this study are coal, coke, gas, gasoline, diesel, kerosene and electricity. All energy consumption data have been converted to standard coal. The formula is as follows.

$$C_{ID} = \sum_i^n EC_i * NHV_i * C_i * O_i * \frac{44}{12} + EPC * \delta \tag{2}$$

where C_{ID} represents carbon emission of built-up land (t). EC_i , NHV_i , C_i and O_i denote the energy consumption, net calorific value (TJ·Gg⁻¹), carbon content and oxidation rate of the i th energy source, respectively. EPC and δ are electric power consumption and power carbon emission coefficient, respectively. The specific carbon emission coefficients for each energy source are listed in Table 3.

Combining C_D and C_{ID} , we use net carbon emission (NCE) to represent the total carbon accounting.

$$NCE = C_D + C_{ID} \tag{3}$$

As an illustration, we specify that carbon emission is positive and carbon sequestration is negative in the NCE calculation. As a result, by combining the direct emissions

Table 2 Carbon emission/sequestration coefficient of land use types

| Land use type | CE | CS |
|-----------------|-------|--------|
| Cultivated land | 0.505 | 0.007 |
| Wood land | - | 0.6125 |
| Grass land | - | 0.021 |
| Water | - | 0.041 |
| Bare land | - | 0.0005 |

Table 3 Carbon emission coefficients of various energy source

| Energy type | Net calorific value(NHV) (TJ·Gg ⁻¹) | Carbon content rate(C) (tC·TJ ⁻¹) | Oxidation rate(O) |
|-------------|---|---|-------------------|
| Coal | 20.908 | 26.37 | 0.93 |
| Coke | 28.435 | 29.43 | 0.93 |
| Gas | 38.931 | 15.32 | 0.99 |
| Gasoline | 43.07 | 18.9 | 0.98 |
| Diesel | 42.652 | 20.2 | 0.98 |
| Kerosene | 43.07 | 19.6 | 0.98 |
| | Carbon emission coefficient (δ) | | |
| Electricity | 0.7935 | | |

of the above land and the indirect emissions of the urban build-up land, we can analyze the spatial distribution and temporal change patterns of historical carbon emissions at the national level.

Carbon emission intensity and carbon emission coefficient of built-up land

Based on the spatiotemporal distribution of national carbon emissions from LULC change and fossil energy consumption, we analyze the regional impacts of natural differences on carbon emissions by introducing the carbon emission intensity (CEI) indicator.

$$CEI = \frac{NCE_i}{A_i} \tag{4}$$

where NCE_i and A_i denote the net carbon emissions and the area of i th province, respectively. The carbon intensity figure is used to reflect the average carbon emissions in each province.

Furthermore, we introduce the carbon emission coefficient (CEC) of urban built-up land to specifically analyze the carbon emission density from energy consumption. CEC is calculated as the ratio of carbon emissions to urban built-up land area.

$$CEC = \frac{C_{ID}^j}{UBA_j} \tag{5}$$

where C_{ID}^j represents the carbon emission caused by energy consumption in the j th province, and UBA_j represents its urban built-up land area.

Spatial autocorrelation analysis

To further explore the spatial distribution and association of carbon emissions, we use the spatial autocorrelation to

measure global and local carbon emissions spatial autocorrelation among provinces and between each province with its neighbors, respectively. Spatial autocorrelation measures the degree of spatial clustering or dispersion in the distribution of phenomena, and is analyzed using the Moran index (Lin et al. 2021). Global spatial correlation of carbon emissions among provinces is calculated as follows.

$$I = \frac{\sum_{i=1}^n \sum_{j=1}^n \omega_{ij} (x_i - \bar{x})(x_j - \bar{x})}{S^2(\sum_i \sum_j \omega_{ij})} \quad (6)$$

where S^2 represents overall weights for the space of aggregation, ω_{ij} denotes the weight between the i th and j th province, x_i and x_j represent their province carbon emission. \bar{x} is global carbon emissions in average. If I is greater than 0, the carbon emission is obvious spatial positive correlation among these provinces. Conversely, there is a spatial negative correlation. Otherwise, if $I = 0$, there's no correlation in space.

To further explore local spatial autocorrelation of carbon emissions, we calculate the spatial correlation between each province and its neighboring provinces using the following equation.

$$I_i = \frac{Z_i}{S^2} \sum_{i \neq k} \omega_{ik} Z_k \quad (7)$$

$$Z_{i,k} = X_{i,k} - \bar{X} \quad (8)$$

where I_i is local Moran's I of the i th province. And $Z_{i,k}$ represents the difference between the carbon emission of the i or k province and the overall average value of the surrounding provinces. S^2 and ω_{ik} denote the variance and weight, respectively.

LULC simulation

On the basis of analyzing the regional spatial heterogeneity of carbon fluxes, this paper selects four typical provinces based on their regional spatial association, carbon emissions and fossil energy consumption, and further simulates and predicts regional carbon fluxes. The land-use expansion pattern represents its capacity for expansion. In this study, we quantitatively characterize the expansion pattern of each land-use type by measuring the change in patch area.

$$SF_i = \frac{\text{Expansion Area}_i}{\sum \text{Expansion Area}} \quad (9)$$

where SF_i and Expansion Area_i represent the spread factor and expansion area of the i th land-use type, respectively.

We use the well-established Fourier series fitting and least squares model to simulate CEC of build-up land. This

simulation is then integrated into the PLUS model to predict future carbon emissions.

We combine the results of both simulations, and then input them into PLUS model for land-use simulation to predict future carbon emissions (Liang et al. 2021a). In this study, the probability of random seeds was determined as 0.01 to simulate future types of land use patches, and the land use transfer parameters were set using the land use transfer matrix.

Result and analysis

Distribution pattern and trend of LULC

In China, the LULC is primarily composed of grassland, woodland and cultivated land (Fig. 2).

We analyzed that LULC changes is over four distinct periods (Fig. 3). The total areas of land conversion within these periods are similar, with respective values of $49.76 \times 10^4 \text{ km}^2$, $49.16 \times 10^4 \text{ km}^2$, $52.91 \times 10^4 \text{ km}^2$ and $51.06 \times 10^4 \text{ km}^2$. The LULC change is dominated by cultivated land, whose area decrease by $644.93 \times 10^4 \text{ km}^2$ (3.1% of the total cultivated land), and is mainly converted into woodland and grassland. The conversion proportion of woodland is smaller, with an average of 16.25%. The area of cultivated land converted to woodland has been increased annually, a trend that reflects China's policy of converting cultivated land back to forests in recent years.

Grassland primarily transitions into cultivated land and bare land, with newly formed cultivated land accounting for an average of 37.57%. The need for cultivated land significantly contributes to the overexploitation of grassland. However, in the process of grassland transformation, its main interaction object is bare land. The area converted from grassland to bare land in the four periods are 64,029.78 km^2 , 57,177.72 km^2 , 71,788.07 km^2 and 84,285.43 km^2 , respectively, indicating that the grassland reclamation and overgrazing have led to the degradation of grassland resources. And the newly generated grassland is also dominated by bare land, with an average of 51.27%. The transformation of bare land into grassland mainly results from rational land use, a consequence of land reclamation efforts.

Compared to other land types, the proportion of urban built-up land (UBL) remains relatively low. However, the area of UBL in China has been growing, with 1.60%, 1.81%, 2.10%, 2.41% and 2.66%, respectively. The primary manifestation is expansion of the central city to the surrounding areas. The transfer of UBL is mainly reflected in the interaction with cultivated land. In the past two decades, the average area of UBL transfer is only 7278.05 km^2 , in which the area converted from cultivated land accounts for 65.86%. The ratio of UBL transferred from cultivated land reached

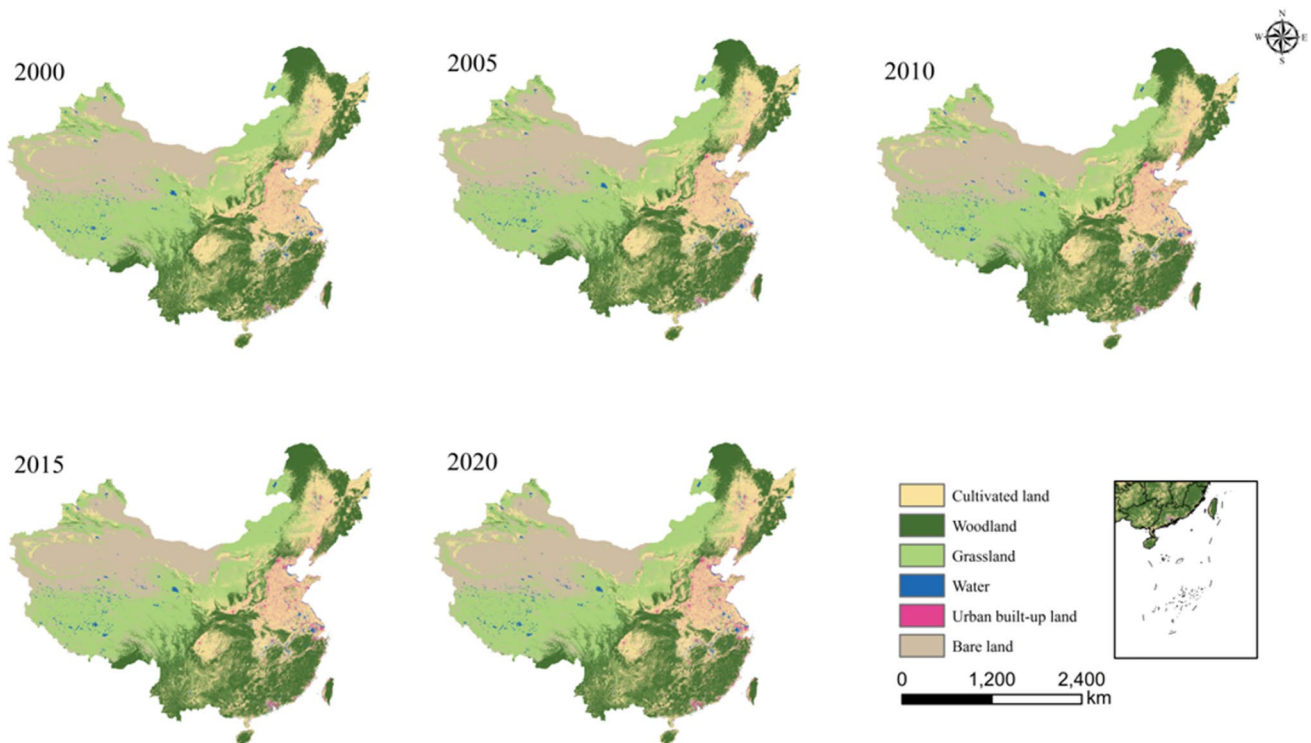


Fig. 2 Spatiotemporal pattern of LULC in China from 2000 to 2020

81.04%. The interaction between UBL and cultivated land is mainly influenced by socio-economic development and human activities. It is necessary to balance the expansion of UBL to meet socio-economic development while preserving China's fundamental permanent farmland.

Spatiotemporal characteristics of provincial carbon emissions

Spatiotemporal dynamic changes of carbon emissions

Figure 4 shows the NCE resulting from LULC and energy consumption. It is evident that national carbon emissions exhibit a continuous growth trend, with variations in emissions caused by LULC among provinces. Over the past two decades, carbon emissions have significantly exceeded carbon sequestration. Carbon emissions are primarily driven by UBL, accounting for 87.75% in 2000 and increasing to 93.84% in 2020. Throughout this period, the contribution of cultivated land in carbon emission is relatively low, staying below 9667.29×10^4 t and keeping a slow decline trend. Therefore, reducing carbon emissions is an effective way to achieve carbon balance. In China's carbon balance system, carbon emissions have a dominant role, and there

is considerable potential to limit UBL carbon emissions through changes in energy activities.

For other land-use types, the contribution degree to carbon sequestration is woodland, grassland, water, and bare land in descending order. Carbon sequestration by woodland is the most significant source of carbon sinks in China's ecosystem, consistently comprising 96.20% in each period, with grassland contributing approximately 2.9%. The contribution of water and bare land to carbon sequestration is almost negligible. Therefore, to achieve carbon balance from a carbon sequestration perspective, rational land planning policies should be implemented to boost carbon sequestration in forest and grasslands and to realize carbon balance in the ecosystem.

Comparisons of carbon emissions and carbon sequestration across provinces reveal a pattern consistent with the overall trend—carbon emissions are invariably higher than sequestration. The provinces with high and rising carbon emissions are primarily located in North China Plain (Hebei, Shandong, Henan). In 2000, the carbon emissions in Shandong were 7951.91×10^4 t. Over the next 10 years, Shandong's carbon emissions ranked first in China, increasing to $12,454.78 \times 10^4$ t in 2010. However, from 2010 to 2015, the growth rate and total emissions in Hebei surpassed that of Shandong, reaching $13,264.99 \times 10^4$ t in 2015, and Hebei has since maintained its first-place position.

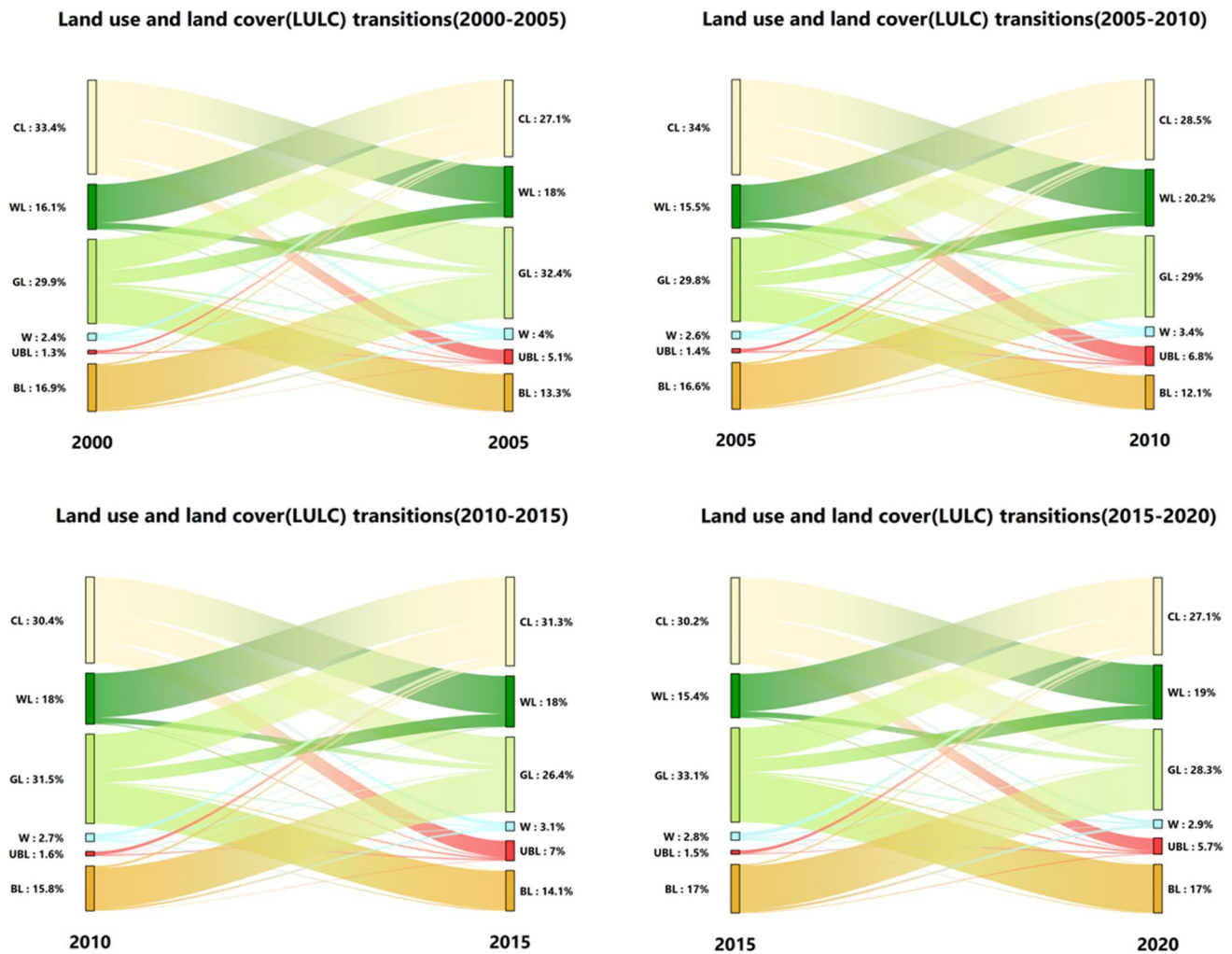


Fig. 3 2000–2020 Inward/outward flow of LULC in China (CL: cultivated land; WL: woodland; GL: grassland; W: water; UBL: urban built-up land; BL: bare land)

Meanwhile, it is noting that, while China's carbon emissions have been increasing, the growth rate has significantly slowed down in each province. Figure 4(f) shows six provinces with high emissions over the past two decades. During the first decade, the growth rate of carbon emissions fluctuated significantly, continuing to rise. From 2010 onwards, carbon emissions in all regions demonstrated a more moderate trend, with negative growth observed in Shandong and Henan. In Shanxi, carbon emissions increased only marginally, while Hebei experienced a growth rate of just 2.6% from 2015 to 2020. Comparing the NCE of 30 provinces over the past 20 years (Fig. 5), we find that the NCE in most regions follows a trend of initial increase followed by a decrease. This trend indicates that government carbon reduction measures to limit human activities and reduce carbon emissions indirectly caused by fossil energy have been effective.

Beyond analyzing carbon emissions and sequestration, we examine carbon emission pressure per unit area across provinces to gain insight into NCE characteristics in each province (Fig. 6). The result shows that overall CEI has not varied significantly. The CEI of the eastern region, especially the coastal provinces, is relatively higher. It's evident that the provinces in the central region with high NCE also have highly CEI. However, for Shanghai and Beijing, while their NCE does not exceed $3318.31 \times 10^4 t$, their carbon emission intensities are relatively high. This indicates a concentrated distribution of industrial production and human activities. It also reveals that Beijing has optimized its energy structure and transferred industries, moving its energy industry to Hebei and reducing its own carbon emissions. A detailed spatial correlation analysis will be described in the "Methodology" section.

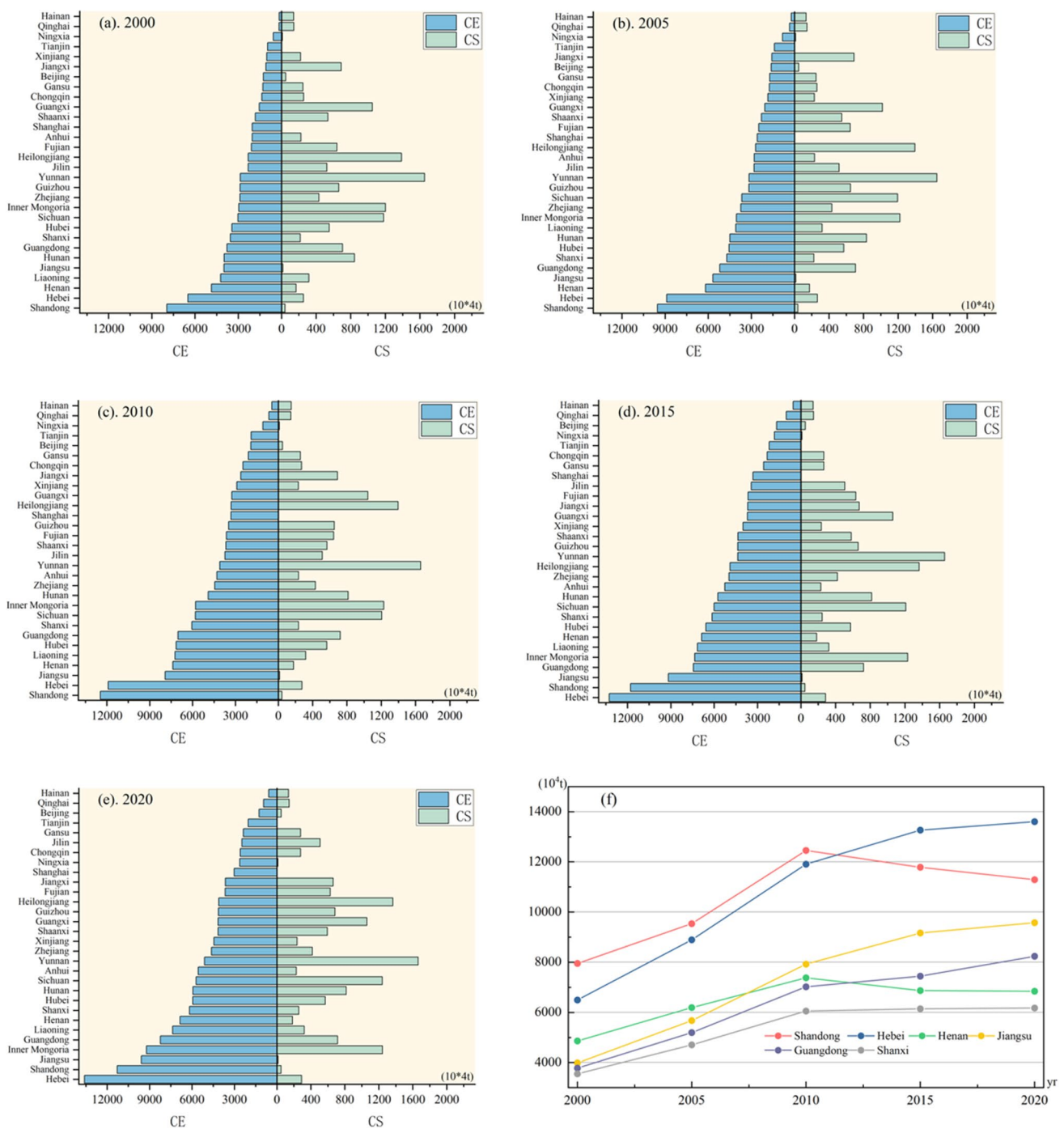


Fig. 4 Changes of carbon emissions by provinces in China and the proportion of carbon emissions in some provinces

Spatial correlation of NCE

As described in the “Spatial correlation of NCE” section, the Moran index is used to further analyze spatial correlations in each region. According to the spatial autocorrelation analysis of China’s NCE from 2000 to 2020 (Table 4), the global carbon emission Moran index in each period is

greater than 0, indicating that the overall NCE in the study area exhibits a positive spatial correlation. The z -values of each year are higher than the 99% confidence level, which is statistically significant. Over the past two decades, the overall Moran has shown a gradually decreasing trend, indicating that the spatial correlation of NCE between different provinces is gradually weakening. The Moran index

Fig. 5 Net carbon emissions at provincial level from 2000 to 2020

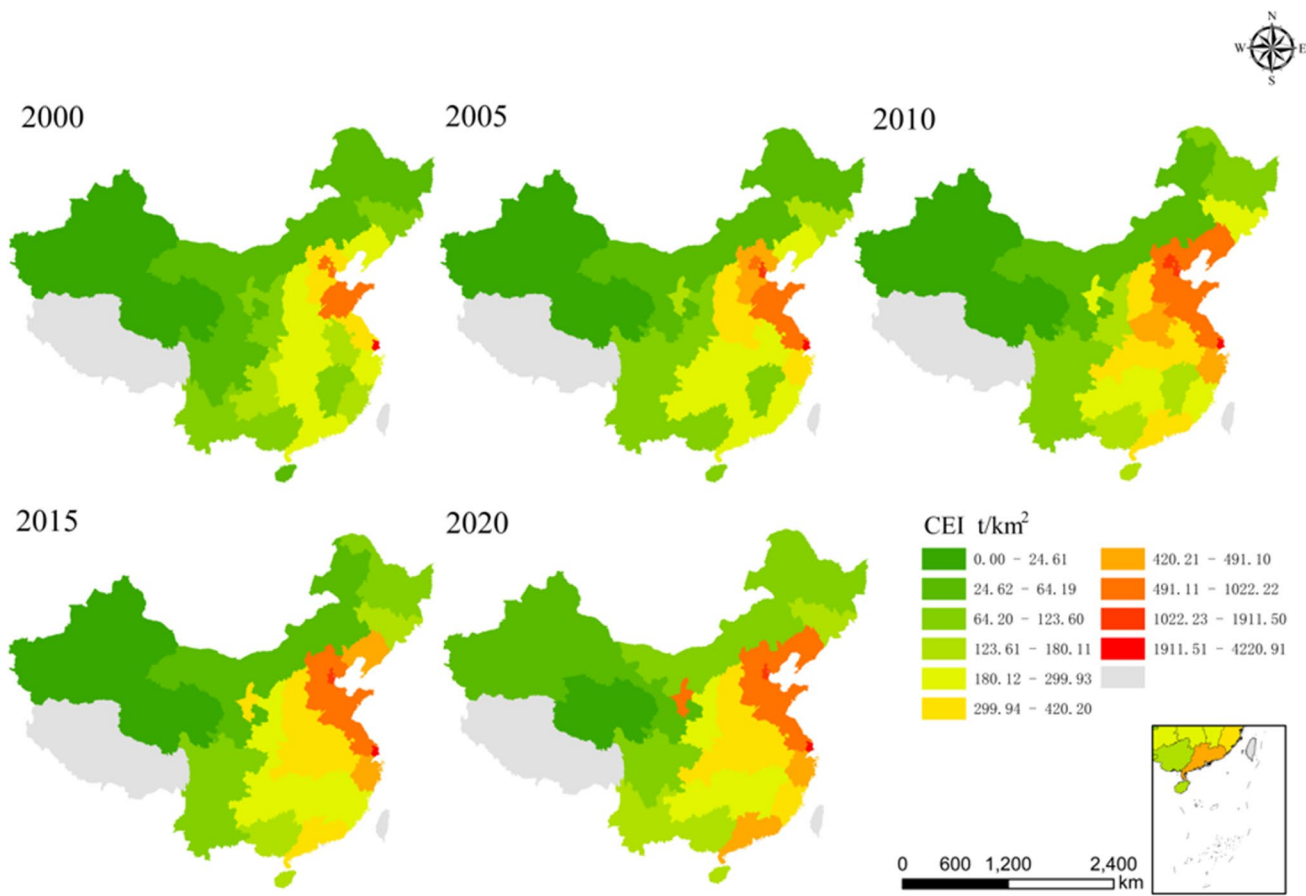
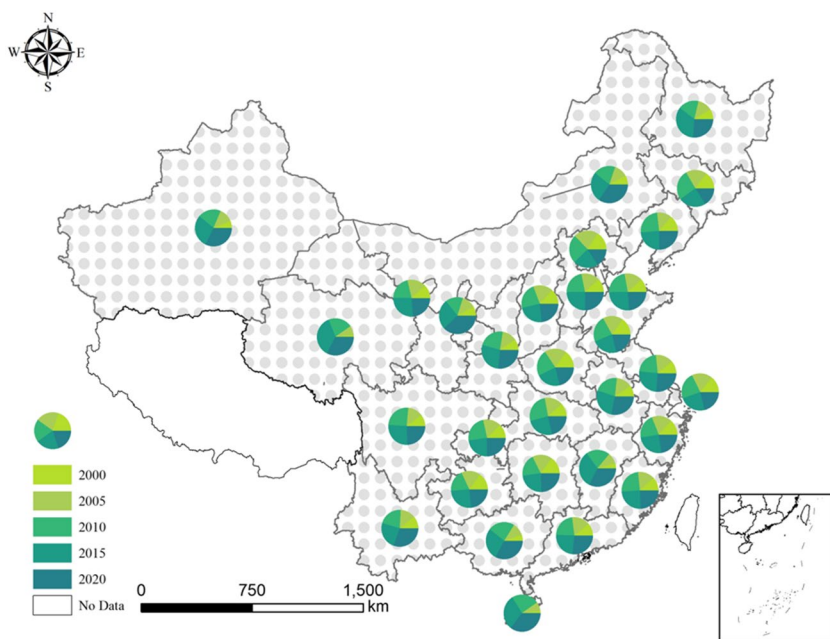


Fig. 6 Carbon emission intensity in China's regions from 2000 to 2020 (t/km^2)

Table 4 The global autocorrelation Moran of carbon emission on land-use in China from 2000 to 2020

| | 2000 | 2005 | 2010 | 2015 | 2020 |
|-----------------|--------|--------|--------|-------|--------|
| <i>p</i> -value | 0.009 | 0.005 | 0.009 | 0.026 | 0.031 |
| <i>z</i> | 2.9829 | 3.0816 | 2.7233 | 2.202 | 2.0646 |
| Moran | 0.317 | 0.311 | 0.283 | 0.211 | 0.2078 |

in 2020 is 0.2078, indicating a continued positive spatial correlation.

The analysis continues by exploring spatial relationships using local carbon emission Moran index. Provinces with significant spatial relationships are categorized into four groups (Fig. 7), “High-High” (HH), “High-Low” (HL), “Low-High” (LH) and “Low-Low” (LL).

High-High (HH) indicates the NCE is high in the objective province and its neighbors, like Hebei.

High-Low (HL) indicates the NCE is high in the objective province but low in its neighbors, like Sichuan in 2015.

Low-High (LH) indicates the NCE is low in the objective province but high in its neighbors, like Anhui and Beijing in 2005 and 2020, respectively.

Low-Low (LL) indicates the NCE is low in the objective province and its neighbors, like Xinjiang and Sichuan in 2020.

The results show that, over the past two decades, the HH and LL provinces made up 90%, 90%, 71.4%, 87.5%, and 88.9% of the total, respectively. The spatial correlation of provincial-level NCE is relatively high, with evident aggregation. Particularly, Sichuan showed an LL pattern initially, but transitioned to an HL pattern in 2010 and 2015. This shift is attributed to increased energy consumption resulting from Sichuan’s urban construction and development during this period, which directly raised UBL carbon emissions. This trend underscores the rapid economic development in Sichuan and its neighboring cities. Beijing, categorized as an LH city, has undergone significant development and transformation in recent years. Many traditional industries in Beijing have transitioned from fossil energy to clean energy. Additionally, the relocation of some enterprises and factories to Hebei has contributed to reduced energy consumption in

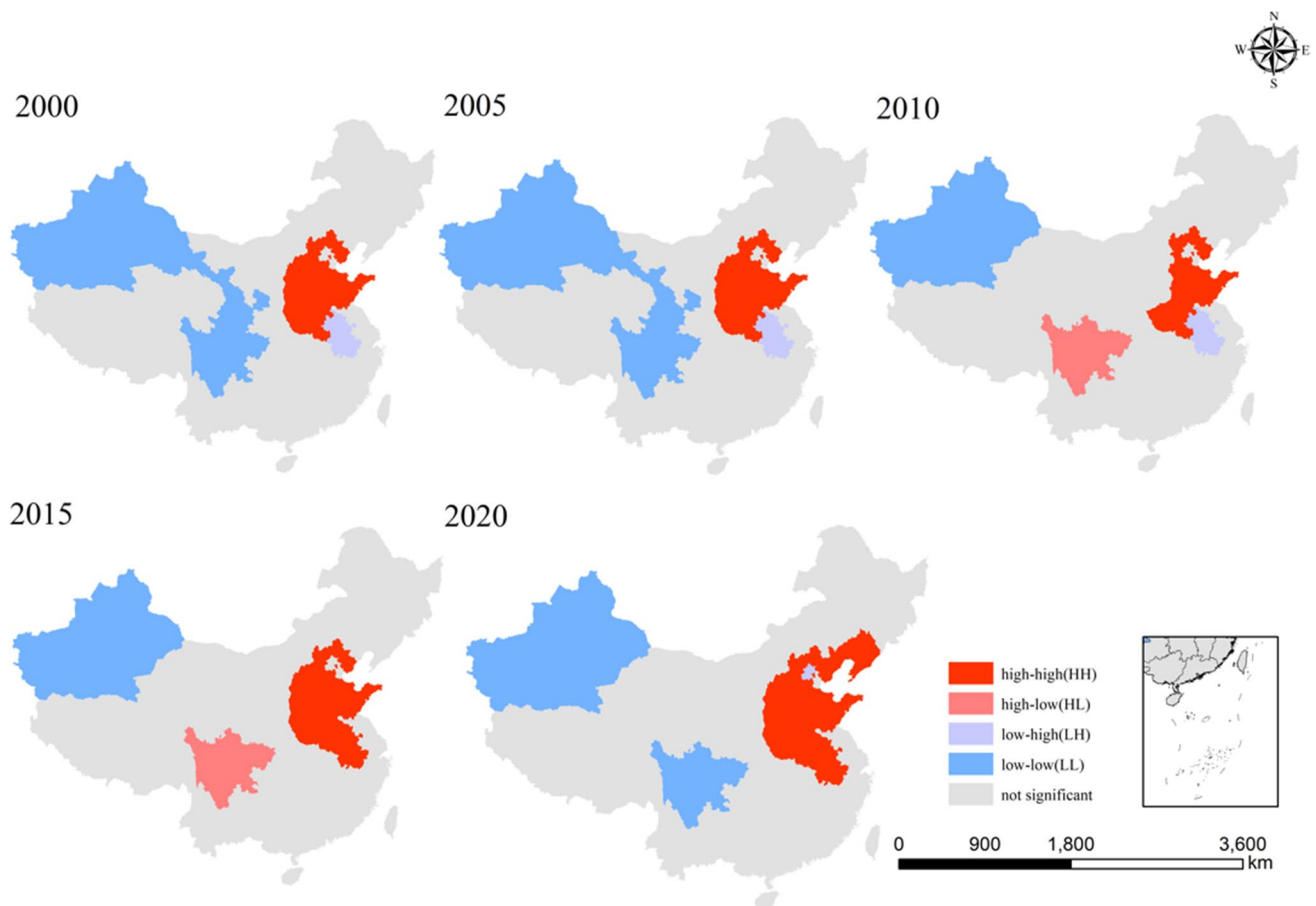


Fig. 7 The LISA (Local Indicators of Spatial Association) spatial agglomeration pattern of NCE in China

Beijing. However, Anhui, shifting from LH to HH, is opposite to Beijing. It is possible that the industrial development in Anhui has overlooked the city's carbon emissions, causing them to rise continuously from 2000 to 2015, with a moderation occurring after 2015.

Simulation of LULC and the carbon emission

Based on the spatiotemporal analysis of provincial carbon emissions, Beijing, Hebei, Anhui, and Sichuan with different spatiotemporal characteristics are selected to explore carbon emissions under future LULC change. This study employs the PLUS model to simulate land-use changes in 2025 and 2030 (Fig. 8).

The results indicate that the LULC of four provinces will not undergo significant changes in the future. The main changes occur among cultivated land, woodland, and UBL. In detail, the cultivated land in Sichuan and Hebei will decrease, with most of it transitioning to woodland. In Sichuan, the UBL is expected to increase, primarily at the expense of cultivated land. The UBL area in Hebei is not expected to see significant changes. Anhui is likely to continue developing around urban areas over the next decade, with the majority of expansion occurring in northern Anhui, driven by the conversion of cultivated land. This trend is expected to be followed by plain areas in the middle and lower reaches of the Yangtze River, while the woodland

areas in southwestern and southeastern Anhui are not anticipated to experience significant changes. In Beijing, the area of cultivated land is projected to decrease, while woodland areas are expected to experience a slight increase. Urban areas, on the other hand, are likely to continue expanding, with most of the growth occurring in the eastern and northern regions. The development of the ecological environment should be considered during urban expansion.

For future carbon emission simulations of UBL, we calculated the carbon density of historical UBL in the four provinces using formula (5) to represent fossil energy consumption levels. We then employed Fourier series fitting and OLS to simulate UBL carbon density by MATLAB Toolbox (Table 5). Fourier fitting is more effective in curve fitting, especially some regions showed a cyclical trend in the short term. We collect two decades of fossil energy data (Fig. 9) and compute the urban area to obtain the UBL carbon density for the simulation. And the results show a relatively well-fitting performance using this method, the adjusted *R*-square are 0.924 (Anhui), 0.947 (Beijing), 0.942 (Hebei), 0.848 (Sichuan), respectively. The results indicate that the carbon density of UBL will continue to decrease over the next decade. The simulation results of carbon accounting in 2025 and 2030 are shown in Table 6 and 7, respectively. The findings reveal that the NCE in 2025 will begin to decrease compared to the previous two decades. The downward trend mainly due to the decline in carbon emissions from UBL,

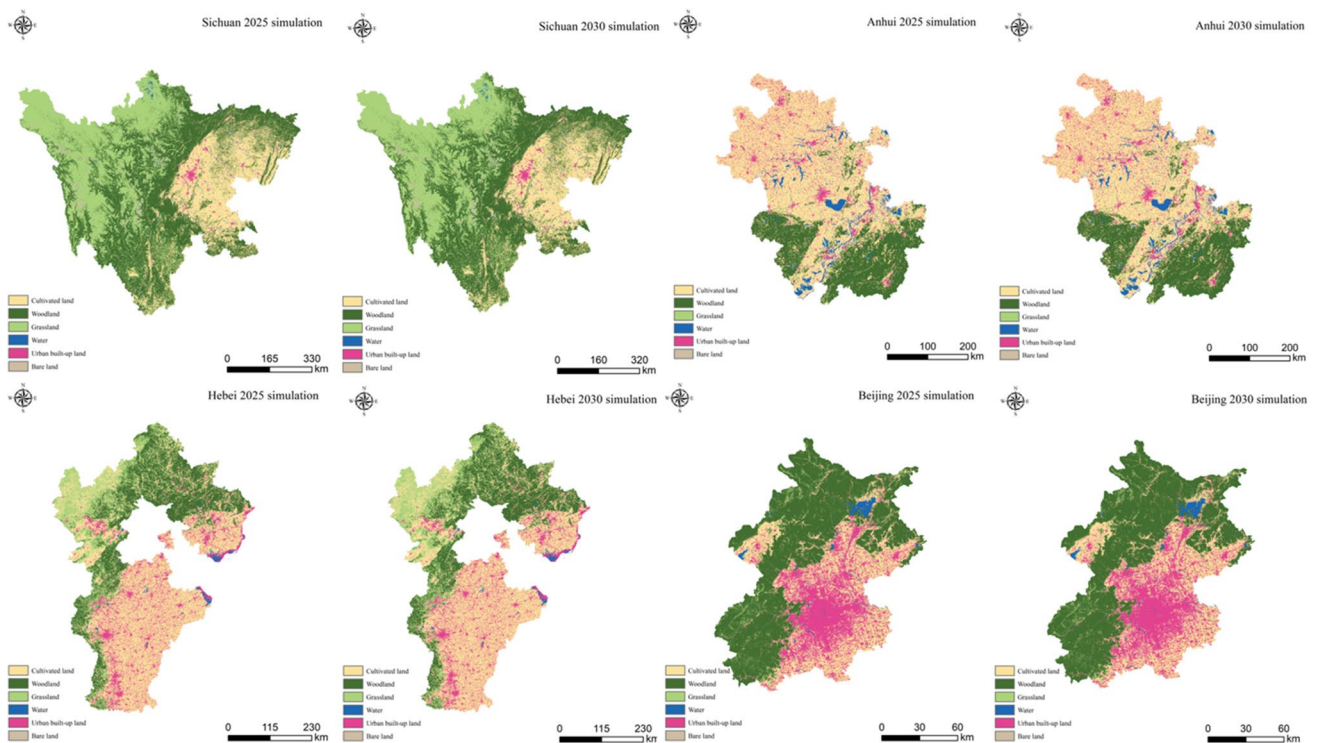


Fig. 8 Typical regional LULC simulation results (2025, 2030)

Table 5 UBL carbon density (t/km²)

| | 2000 | 2005 | 2010 | 2015 | 2020 | 2025 | 2030 |
|---------|-----------|-----------|-----------|----------|-----------|----------|---------|
| Anhui | 2415.18 | 3344.51 | 4661.47 | 4944.97 | 4793.21 | 4341 | 3378.82 |
| Beijing | 5894.46 | 6170.23 | 6333.21 | 4916.39 | 3539.69 | 2658.76 | 1139.41 |
| Hebei | 4378.73 | 5623.86 | 6706.52 | 6524.76 | 6165.63 | 4985.84 | 3196.84 |
| Sichuan | 15,254.72 | 15,460.38 | 20,307.52 | 16,184.2 | 12,859.41 | 10,988.7 | 6777.52 |

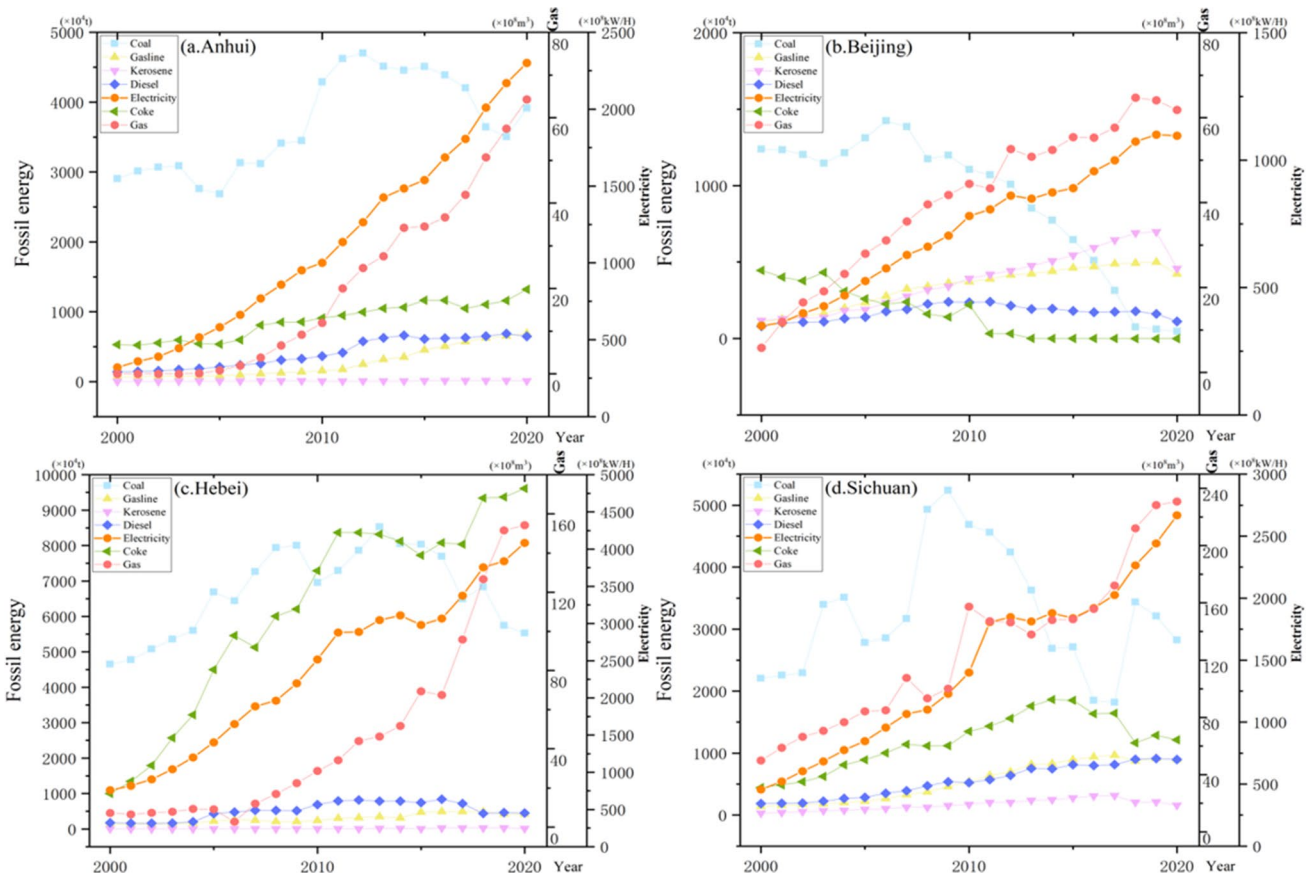


Fig. 9 Specific fossil energy consumption scenarios in four provinces

Table 6 Carbon accounting of land-use types in four provinces in 2025 (t)

| | Cultivated land | Woodland | Grassland | Water | UBL | Bare land |
|---------|------------------------|--------------------------|------------------------|------------|---------------------------|-----------|
| Anhui | 469.75×10 ⁴ | -254.27×10 ⁴ | -54.71 | -30826.55 | 7035.60×10 ⁴ | -0.51 |
| Beijing | 22.31×10 ⁴ | -54.11×10 ⁴ | -841.32 | -1083.14 | 1082.01×10 ⁴ | -0.26 |
| Hebei | 414.14×10 ⁴ | -281.83×10 ⁴ | -6.46×10 ⁴ | -6289.69 | 13,000.90×10 ⁴ | -19.96 |
| Sichuan | 536.35×10 ⁴ | -1225.63×10 ⁴ | -33.77×10 ⁴ | -15,254.99 | 5692.84×10 ⁴ | -2952.58 |

Table 7 Carbon accounting of land-use types in four provinces in 2030 (t)

| | Cultivated land | Woodland | Grassland | Water | UBL | Bare land |
|---------|------------------------|--------------------------|------------------------|------------|-------------------------|-----------|
| Anhui | 467.93×10 ⁴ | -251.54×10 ⁴ | -48.22 | -29640.13 | 5849.34×10 ⁴ | -0.51 |
| Beijing | 21.64×10 ⁴ | -54.24×10 ⁴ | -835.59 | -1115.82 | 476.00×10 ⁴ | -0.21 |
| Hebei | 412.19×10 ⁴ | -287.13×10 ⁴ | -6.39×10 ⁴ | -5894.78 | 8323.47×10 ⁴ | -15.45 |
| Sichuan | 519.57×10 ⁴ | -1251.00×10 ⁴ | -33.43×10 ⁴ | -15,468.93 | 3933.60×10 ⁴ | -3037.41 |

while the carbon emissions from cultivated land also will decrease. For other land-use types, woodland is still the land type with the highest carbon sequestration contribution, followed by water and grassland.

At the provincial level, we compare historical and simulated carbon data. Although the carbon density of UBL in Anhui has begun to decrease in 2025, its overall carbon emissions are still rising due to the rapid development of UBL areas. The carbon emissions from UBL will not start decreasing until 2030. The rapid urban development of Anhui may introduce a large amount of fossil energy consumption from the surrounding provinces. Consequently, Anhui's carbon emissions continue to increase, while the emissions of surrounding cities may decrease in the future. Beijing's carbon emissions will continue to decline in the next 10 years. Although its NCE remains above 0, it is already significantly lower than in other provinces. It is predicted that Hebei's carbon emissions will remain at $13,126.13 \times 10^4 \text{t}$ in 2025. Its NCE will remain almost unchanged and will begin to decline after 2025.

In conjunction with the earlier spatial correlation findings, our analysis is validated. Beijing has greatly reduced the consumption of fossil energy through energy transformation and factory transfer. It has helped it reduce carbon emissions. The transferred enterprises and factories might not be fully integrated until after 2025, at which point Hebei's carbon emissions are expected to continue decreasing. Sichuan stands out from other regions in terms of its land-use composition. The predominant land-use types are woodland and grassland, collectively making up 74.63% of the province's area. Even though UBL has high carbon density, it occupies a small land area, and while the extensive woodlands and grasslands contribute significantly to carbon sequestration. As a result, Sichuan's NCE is lower compared to other provinces. Over the next decade, the ongoing expansion of forests and grasslands, coupled with Sichuan's energy transition will further reduce its carbon emissions.

Discussion

Land-use and carbon emissions/sequestrations reduction strategies

The land-use system is an extremely complex ecosystem, but it is also highly susceptible to the influence of human activities on its evolutionary process (IPCC Climate Change 2022; Wang et al. 2014). In this paper, we have assessed the historical carbon emission trends in terms of annual carbon emissions/sequestrations by the carbon flows between land-use and fossil energy from human activities in an integrated manner. Under human influence, while negative feedbacks from fossil energy-induced carbon emissions are

more influential, positive feedbacks from land-use in terms of carbon sequestrations are also indispensable. Therefore, when considering coupled human-land development, it's essential to include carbon emissions and sequestrations generated by both land-use and human activities in the assessment to achieve optimal planning (Houghton 2003). Despite the results showing a year-by-year increase in China's carbon emissions, it is not difficult to realize that the emission reduction of fossil energy focuses on coal through the energy emissions of the four provinces. It is relatively uncomplicated to reduce carbon emissions by limiting fossil energy consumption (Fig. 9).

However, land-use as another important form of mitigating carbon emissions is an important consideration to be emphasized. According to our results, expansion of woodland contributes to the reduction of carbon emissions, and woodland as the carbon sequestration should be prioritized when considering the optimization of the land-use structure. Secondly, land-use results over the past two decades show that UBL has been expanding, yet this land use patterns are not conducive to emission reduction strategies. Therefore, this paper subsequently enhances the approach on carbon reduction strategies by introducing carbon emission simulations.

Currently, the simulation analysis of carbon emissions is mainly based on fossil energy, however, it is not enough to consider the impact of fossil energy alone. In this paper, the PLUS model is chosen to simulate future land-use development and carbon emissions/sequestrations, which can help decision makers to develop reasonable land use management and carbon reduction strategies.

In our experiments under a natural development scenario, we observed a decreasing trend in the carbon intensity of UBL across the four typical regions in the future. In fact, the carbon intensity of UBL depends not only on the level of fossil energy consumption, but also on the area of UBL within the study region. Therefore, the change in the area of UBL is another factor of concern during land-use simulation. The carbon emission simulation results indicate that carbon emissions will decrease in all regions in the future, albeit at varying rates. The observed trend in carbon emission mitigation aligns with China's future policies, which advocate for energy upgrading and transformation, prioritizing compact urban growth and afforestation, and optimizing land-use structures and urban growth patterns to reduce carbon emissions.

Uncertainty

This study has limitations that need to be addressed and refined in future research. First, we used a 1-km resolution for our carbon source and sequestration experiments, which ignored some rural areas or small villages of UBL, which

may lead to small carbon emission results of UBL in the subsequent carbon emission simulation. Second, this study focused solely on the relationship between the study area's size and carbon emissions, neglecting the impact of socio-economic factors like population and GDP. Future research should take these factors into account for a more comprehensive analysis. Lastly, our land-use carbon emission only considered the trend of carbon emissions in 2025 and 2030 under a natural scenario. In future research, we plan to evaluate carbon emission trends in China under multiple scenarios, starting with optimizing the land-use structure.

Conclusion

In this study, we analyze the patterns of overall carbon emissions in thirty provinces of China over the past two decades, considering land-use distribution and fossil energy consumption. Based on this analysis, we provide reference suggestions for optimizing land-use structure, upgrading and transforming fossil energy, and promoting low carbon emission development in China. Driven by global warming and rapid socio-economic development, China has experienced intensified changes in its land-use structure and fossil energy consumption, leading to a surge in carbon emissions. In 2020, the Chinese government introduced the dual carbon target at the United Nations General Assembly. Studying changes in land-use and fossil energy can proactively contribute to achieving this target. This study accounts for the carbon source/sequestration and spatial relationship in China based on land-use data from 2000 to 2020 and fossil energy consumption data for the past two decades. The study concludes that China's carbon emissions have generally increased over the past two decades, with significant variations among provinces. However, the overall carbon emission increase rate has been decreasing, and part of the provinces has already showed negative carbon emission growth. The overall spatial aggregation relationship exhibits a positive correlation, with some provinces showing significant clustering in local areas. As a result, we have selected four representative provinces to conduct carbon emission simulations to project the development trends of carbon emissions over the next ten years and analyze the reasons for their prominence in local spatial correlation. Our carbon emission prediction experiments indicate that some provinces are already expected to experience carbon emission reductions in the future, primarily due to a decrease in carbon emissions exported by UBL. While the area of UBL in the four provinces is projected to continue increasing trend over the next decade, the overall carbon emission density of built-up land is expected to decrease, largely due to reduced fossil energy consumption and the potential for a higher proportion of clean energy input. Consequently, overall carbon emission

is anticipated to decrease. This study may have overlooked the correlations with larger region. Future research should comprehensively consider overall regional carbon emissions and their intrinsic linkages. In addition, more specific factors and scenarios can be considered to improve the accuracy of carbon emission accounting.

Author contribution Yuxiang Cheng: Writing original draft, conceptualization, funding acquisition, project administration, formal analysis, and supervision. Yuqi Tang: writing original draft, methodology, literature review, data curation, visualization, and supervision. Bin Zou: writing, review, editing, visualization, and validation. Huihui Feng: resources, data curation, and supervision.

Funding This research was supported by the National Natural Science Foundation of China (Grant 41971313); the National Natural Science Foundation of China (Grant 42271411); Research Project on Monitoring and Early Warning Technologies for Implementation of Land Use Planning in Guangzhou City (2020B0101130009); Open Fund of Key Laboratory of Urban Land Resources Monitoring and Simulation, Ministry of Natural Resources [No. KF-2022-07-021].

Data availability The datasets used and/or analyzed during the current study are available from the corresponding author on reasonable request.

Declarations

Competing interests The authors declare no competing interests.

References

- Brovkin V, Boysen L, Arora VK et al (2013) Effect of anthropogenic land-use and land-cover changes on climate and land carbon storage in CMIP5 projections for the twenty-first century. *J Clim* 26(18):6859–6881
- Chuai XW, Huang XJ, Zheng ZQ (2011) Impacts of land use change on carbon storage of terrestrial ecosystem in Jiangsu province. *J Res Sci* 33:1932–1939
- Chuai X, Huang X, Wang W et al (2015) Land use, total carbon emissions change and low carbon land management in Coastal Jiangsu, China. *J Clean Prod* 103:77–86
- Dietz J, Treydte AC, Lippe M (2023) Exploring the future of Kafue National Park, Zambia: Scenario-based land use and land cover modelling to understand drivers and impacts of deforestation. *Land Use Policy* 126:106535. <https://doi.org/10.1016/j.landusepol.2023.106535>
- Dong F, Dai YJ, Zhang SN et al (2019) Can a carbon emission trading scheme generate the Porter effect? Evidence from pilot areas in China. *Sci Total Environ* 653:565–577
- Field, Behrenfeld, Randerson et al (1998) Primary production of the biosphere: integrating terrestrial and oceanic components. *Science* (new York, n.y.) 281(5374):237–240
- Guo X, Chuai X, Huang X (2019) A land use/land cover based green development study for different functional regions in the Jiangsu Province, China. *Int J Environ Res Public Health* 16(7):1277. <https://doi.org/10.3390/ijerph16071277>
- Han X, Yu J, Xia Y et al (2021) Spatiotemporal characteristics of carbon emissions in energy-enriched areas and the evolution of regional types. *Energy Rep* 7:7224–7237

- He CY, Zhang D, Huang QX et al (2016) Assessing the potential impacts of urban expansion on regional carbon storage by linking the LUSD-urban and InVEST models. *Environ Model Softw* 75:44–58
- Hong CP, Burney JA, Pongratz J et al (2021) Global and regional drivers of land-use emissions in 1961–2017. *Nature* 589(7843):554
- Houghton RA, Hackler JL (2003) Sources and sinks of carbon from land-use change in China. *Global Biogeochem Cycles* 17(2):1034. <https://doi.org/10.1029/2002GB001970>
- Houghton RA (2003) Revised estimates of the annual net flux of carbon to the atmosphere from changes in land use and land management 1850–2000. *Tellus B: Chem Phys Meteorol* 55(2):378–390. <https://doi.org/10.3402/tellusb.v55i2.16764>
- Huang HZ, Jia JS, Zhang ZX (2023) Spatiotemporal pattern evolution and influence factors of land-use carbon emissions in counties, Jiangxi Province. *Acta Ecol Sin* 43(20):8390–8403. <https://doi.org/10.20103/j.stxb.202211293454>
- IPCC Climate Change (2022) Impacts, adaptation, and vulnerability. contribution of working group II to the sixth assessment report of the intergovernmental panel on climate change. [Pörtner H-O, Roberts DC, Tignor M, Poloczanska ES, Mintenbeck K, Alegria A, Craig M, Langsdorf S, Löschke S, Möller V, Okem A, Rama B (eds.)]. Cambridge University Press. Cambridge University Press, Cambridge, UK and New York, NY, USA, pp. 3056. <https://doi.org/10.1017/9781009325844>. .
- Jung M et al (2012) Global patterns of land-atmosphere fluxes of carbon dioxide, latent heat, and sensible heat derived from eddy covariance, satellite, and meteorological observations. *J. Geophys. Res.* 117:G04011. <https://doi.org/10.1029/2012JG002190>
- Lai L, Huang XJ, Yang H et al (2016) Carbon emissions from land-use change and management in China between 1990 and 2010. *Sci Adv* 2(11):e1601063. <https://doi.org/10.1126/sciadv.1601063>
- Le Quere C, Raupach MR, Canadell JG et al (2009) Trends in the sources and sinks of carbon dioxide. *Nat Geosci* 2(12):831–836
- Li H, Zhao Y, Wang S et al (2020) Spatial-temporal characteristics and drivers of the regional residential CO₂ emissions in China during 2000–2017. *J Clean Prod* 276:124116. <https://doi.org/10.1016/j.jclepro.2020.124116>
- Li M, Zhang YF, Liu HC (2022a) Carbon neutrality in Shanxi Province: scenario simulation based on LEAP and CA-Markov models. *Sustainability* 14(21):13808. <https://doi.org/10.3390/su142113808>
- Li S, Cao Y, Liu J et al (2022b) Assessing spatiotemporal dynamics of land use and cover change and carbon storage in China's ecological conservation pilot zone: a case study in Fujian Province. *Remote Sens* 14(16):4111. <https://doi.org/10.3390/rs14164111>
- Liang X, Guan QF, Clarke KC et al (2021a) Understanding the drivers of sustainable land expansion using a patch-generating land use simulation (PLUS) model: a case study in Wuhan, China. *Comput Environ Urban Syst* 85:101569. <https://doi.org/10.1016/j.compevnurbysys.2020.101569>
- Liang Y, Hashimoto S, Liu L (2021b) Integrated assessment of land-use/land-cover dynamics on carbon storage services in the Loess Plateau of China from 1995 to 2050. *Ecol Ind* 120:106939. <https://doi.org/10.1016/j.ecolind.2020.106939>
- Lin Q, Zhang L, Qiu B et al (2021) Spatiotemporal analysis of land use patterns on carbon emissions in China. *Land* 10(2):141. <https://doi.org/10.3390/land10020141>
- Lorenz R, Pitman AJ (2014) Effect of land-atmosphere coupling strength on impacts from Amazonian deforestation. *Geophys Res Lett* 41(16):5987–5995
- Luyssaert S, Schulze ED, Börner A et al (2008) Old-growth forests as global carbon sinks. *Nature* 455(7210):213–215
- Mallick J, Almesfer MK, Alsubih M et al (2022) Estimating carbon stocks and sequestration with their valuation under a changing land use scenario: a multi-temporal research in Abha City, Saudi Arabia. *Front Ecol Evol* 10:905799. <https://doi.org/10.3389/fevo.2022.905799>
- Molotoks A, Stehfest E, Doelman J et al (2018) Global projections of future cropland expansion to 2050 and direct impacts on biodiversity and carbon storage. *Glob Change Biol* 24(12):5895–5908
- Pechanec V, Purkyt J, Benc A et al (2018) Modelling of the carbon sequestration and its prediction under climate change. *Eco Inform* 47:50–54
- Piao SL, Fang JY, Ciais P et al (2009) The carbon balance of terrestrial ecosystems in China. *Nature* 458(7241):1009–U82
- Smith P, Martino D, Cai Z et al (2008) Greenhouse gas mitigation in agriculture. *Philos Trans R Soc B-Biol Sci* 363(1492):789–813
- Su YX, Chen XZ, Li Y et al (2014) China's 19-year city-level carbon emissions of energy consumptions, driving forces and regionalized mitigation guidelines. *Renew Sustain Energy Rev* 35:231–243
- Tao Y, Li F, Wang R et al (2015) Effects of land use and cover change on terrestrial carbon stocks in urbanized areas: a study from Changzhou, China. *J Clean Prod* 103:651–657
- Wang L, Ma D, Chen W (2014) Future CO₂ emissions allowances and inequality assessment under different allocation regimes. *Energy Procedia* 61:523–526
- Wang CY, Myint SW (2016) Environmental concerns of deforestation in Myanmar 2001–2010. *Remote Sens* 8(9):728. <https://doi.org/10.3390/rs8090728>
- Yang J, Huang X (2021) The 30 m annual land cover dataset and its dynamics in China from 1990 to 2019. *Earth Syst Sci Data* 13(8):3907–3925
- Yang X, Jin X, Xiang X et al (2018) Carbon emissions induced by farmland expansion in China during the past 300 years. *Sci China Earth Sci* 62(2):423–437
- Yang J, Li Y, Hay I et al (2019) Decoding national new area development in China: toward new land development and politics. *Cities* 87:114–120
- Zhang L, Lin X, Xiao Y et al (2023) Spatial and structural characteristics of the ecological network of carbon metabolism of cultivated land based on land use and cover change: a case study of Nanchang, China. *Environ Sci Pollut Res Int* 30(11):30514–30529
- Zhang DJ, Ge WY, Zhang Y (2020) Evaluating the vegetation restoration sustainability of ecological projects: a case study of Wuqi county in China. *J Clean Prod* 264:121750. <https://doi.org/10.1016/j.jclepro.2020.121751>
- Zhao C, Liu Y, Yan Z (2023) Effects of land-use change on carbon emission and its driving factors in Shaanxi Province from 2000 to 2020. *Environ Sci Pollut Res Int* 30(26):68313–68326

Publisher's Note Springer Nature remains neutral with regard to jurisdictional claims in published maps and institutional affiliations.

Springer Nature or its licensor (e.g. a society or other partner) holds exclusive rights to this article under a publishing agreement with the author(s) or other rightsholder(s); author self-archiving of the accepted manuscript version of this article is solely governed by the terms of such publishing agreement and applicable law.